



Published in final edited form as:

Sci Transl Med. 2013 January 30; 5(170): 170ra14. doi:10.1126/scitranslmed.3005123.

Binge Drinking Induces Whole-Body Insulin Resistance by Impairing Hypothalamic Insulin Action

Claudia Lindtner¹, Thomas Scherer^{1,2}, Elizabeth Zielinski¹, Nika Filatova¹, Martin Fasshauer¹, Nicholas K. Tonks³, Michelle Puchowicz⁴, and Christoph Buettner^{1,5,*}

¹Department of Medicine, Icahn School of Medicine at Mount Sinai, One Gustave L. Levy Place, New York, NY 10029-6574, USA

²Division of Endocrinology and Metabolism, Department of Internal Medicine III, Medical University of Vienna, Waehringer Guertel 18-20, 1090 Vienna, Austria

³Cold Spring Harbor Laboratory, 1 Bungtown Road, Cold Spring Harbor, NY 11724, USA

⁴Mouse Metabolic Phenotyping Center, Case Western Reserve University, 10900 Euclid Avenue, Cleveland, OH 44106, USA

⁵Department of Neuroscience and Diabetes, Obesity and Metabolism Institute (DOMI), Icahn School of Medicine at Mount Sinai, New York, NY 10029-6574, USA

Abstract

Individuals with a history of binge drinking have an increased risk of developing the metabolic syndrome and type 2 diabetes. Whether binge drinking impairs glucose homeostasis and insulin action is unknown. To test this, we treated Sprague-Dawley rats daily with alcohol (3 g/kg) for three consecutive days to simulate human binge drinking and found that these rats developed and exhibited insulin resistance even after blood alcohol concentrations had become undetectable. The animals were resistant to insulin for up to 54 hours after the last dose of ethanol, chiefly a result of impaired hepatic and adipose tissue insulin action. Because insulin regulates hepatic glucose

*To whom correspondence should be addressed. christoph.buettner@mssm.edu.

SUPPLEMENTARY MATERIALS

www.sciencetranslationalmedicine.org/cgi/content/full/5/170/170ra14/DC1

Fig. S1. Serum alcohol levels 1 hour, 8 hours (before GTT), and 9 hours (steady state of basal pancreatic clamp) after last ethanol injection in female rats.

Fig. S2. Glucose tolerance in female rats 8 hours after oral gavage binge drinking model.

Fig. S3. GTTs in male rats subjected to binge drinking ethanol model.

Fig. S4. Plasma insulin levels from female rats during a GTT after binge drinking.

Fig. S5. Hepatic insulin signaling in female rats assessed by Western blot after a hyperinsulinemic pancreatic clamp.

Fig. S6. Hepatic glucose production and insulin levels in female rats subjected to a hyperinsulinemic pancreatic clamp protocol 30 hours after binge drinking.

Fig. S7. Plasma insulin, body weight, and food intake in female rats centrally infused with vehicle, PS1145, or CPT-157633 and subjected to binge drinking model.

Fig. S8. Serum alanine aminotransferase (ALT) and aspartate aminotransferase (AST) concentrations before hyperinsulinemic pancreatic clamp.

Table S1. Plasma nonesterified free fatty acids (NEFAs) from female rats during hyperinsulinemic (3 mU) and basal (0.8 mU) pancreatic clamp studies.

Table S2. Plasma triglycerides from female rats during hyperinsulinemic (3 mU) and basal (0.8 mU) pancreatic clamp studies.

Author contributions: C.L., T.S., E.Z., N.F., and M.F. performed the experiments, data acquisition, analysis, and interpretation; T.S. helped with the drafting of the manuscript; M.P. performed mass spectrometry analysis and helped with interpretation of data and drafting of the manuscript; N.K.T. provided the PTP1B inhibitor and helped with interpretation of data and drafting of the manuscript; C.L. and C.B. designed the study, performed analysis and interpretation of the data, and wrote the manuscript; C.B. supervised the study.

Competing interests: The authors declare that they have no competing interests.

production and white adipose tissue lipolysis, in part through signaling in the central nervous system, we tested whether binge drinking impaired brain control of nutrient partitioning. Rats that had consumed alcohol exhibited impaired hypothalamic insulin action, defined as the ability of insulin infused into the mediobasal hypothalamus to suppress hepatic glucose production and white adipose tissue lipolysis. Insulin signaling in the hypothalamus, as assessed by insulin receptor and AKT phosphorylation, decreased after binge drinking. Quantitative polymerase chain reaction showed increased hypothalamic inflammation and expression of protein tyrosine phosphatase 1B (PTP1B), a negative regulator of insulin signaling. Intracerebroventricular infusion of CPT-157633, a small-molecule inhibitor of PTP1B, prevented binge drinking-induced glucose intolerance. These results show that, in rats, binge drinking induces systemic insulin resistance by impairing hypothalamic insulin action and that this effect can be prevented by inhibition of brain PTP1B.

INTRODUCTION

Binge drinking, which is defined as the consumption of five drinks of alcohol within 2 hours in men or four drinks in women, once a month or more often is associated with an increased risk for developing the metabolic syndrome and type 2 diabetes (1–4). This is a particular public health concern because the incidence of binge drinking continues to rise, especially in the young population (5–7). Insulin resistance is a core characteristic of patients with the metabolic syndrome and type 2 diabetes. It is not known whether the epidemiological association between binge drinking and the metabolic syndrome and type 2 diabetes is causal (that is, binge drinking induces insulin resistance) or whether insulin resistance develops secondary to increased caloric intake as a result of, for example, alterations in central reward pathways (8). Moreover, in one study, binge drinking was associated with type 2 diabetes in individuals that binge drink as rarely as once a month. It is therefore possible that binge drinking induces metabolic derangements that persist after alcohol has been metabolized and cleared from the system (1). Insulin stimulates glucose uptake and utilization in muscle and fat while suppressing glucose production (GP) in the liver and adipose tissue lipolysis. Insulin controls hepatic GP (hGP) by acting on hepatocytes and by decreasing gluconeogenic substrate flux to the liver, in part through antilipolytic effects (9). In addition, insulin controls autonomic nervous system outflow to the liver (10) and adipose tissue (11) through signaling in the central nervous system, thereby restraining hGP and fatty acid release. Impaired insulin action in a particular organ can be caused by diminished insulin signaling in that organ or by impaired inter-organ cross talk or both (12, 13).

Insulin signaling is tightly controlled by tyrosine phosphatases that dephosphorylate the insulin receptor and downstream signaling mediators such as insulin receptor substrate 1 (IRS1). One important mediator is protein tyrosine phosphatase 1B (PTP1B), a negative regulator of insulin and leptin signaling (14). PTP1B is encoded by *PTPN1*, and single-nucleotide polymorphisms in the *PTPN1* gene are associated with type 2 diabetes and obesity (15, 16). PTP1B-deficient mice show increased insulin sensitivity and decreased adiposity, and are protected from diet-induced obesity (17, 18). A similar phenotype is observed in mice that lack PTP1B only in the central nervous system (19), indicating that brain PTP1B is a major regulator of energy homeostasis.

Insulin signaling in the hypothalamus suppresses hGP and white adipose tissue (WAT) lipolysis. In obese humans, or those with type 2 diabetes, insulin is less able to suppress GP and lipolysis, which by definition represents insulin resistance (20, 21). Genetic manipulations that impair insulin signaling in the hypothalamus of rodents can lead to systemic insulin resistance (22). Further, overfeeding can impair hypothalamic insulin action in rodents even before there is any increase in adiposity, resulting in the failure of insulin

infused into the central nervous system to suppress hGP and WAT lipolysis (12, 23). Thus, impaired hypothalamic insulin action in type 2 diabetes and obesity alters the central nervous system control of nutrient partitioning in target organs such as adipose tissue and liver. Increased PTP1B, hypothalamic inflammation, and endoplasmic reticulum stress in the hypothalamus can impair hypothalamic insulin action by inhibiting insulin signaling (24–27). Additionally, elevated endocannabinoid concentrations in the central nervous system impair brain insulin action, likely by acting as a retrograde inhibitor of synaptic transmission (12).

Acute and chronic ethanol exposure leads to functional insulin resistance, measured as the inability of systemic insulin to suppress lipolysis and insulin-stimulated glucose uptake (28, 29). Yet, paradoxically, ethanol also enhances hepatic insulin receptor phosphorylation and downstream protein kinase B (AKT) signaling (30). Thus, the pathophysiology and the molecular defects inducing alcohol-induced insulin resistance remain poorly understood (29, 31, 32). Here, we explored mechanisms through which binge drinking impairs peripheral and central insulin action in rats.

RESULTS

Binge drinking impairs glucose homeostasis in rats

To assess whether binge drinking alters glucose homeostasis, we administered ethanol (3 g/kg) daily for three consecutive days through intraperitoneal injection or orally through gavage to female or male Sprague-Dawley (SD) rats, an established rat model of binge drinking (Fig. 1A) (33–35). Rats in the control group received either saline or an isocaloric glucose solution as indicated and were pair-fed to match caloric intake between groups. Alcohol was undetectable in blood 8 hours after the last ethanol administration on the third day (fig. S1A), at which point animals were subjected to an intraperitoneal glucose tolerance test (GTT). Independent of the route of administration (fig. S2A), ethanol treatment impaired glucose tolerance in comparison to controls, in both female and male rats (Fig. 1B and fig. S3, A to C). Plasma insulin concentrations were higher in the ethanol-treated group after fasting and throughout the GTT, suggesting that insulin resistance may have been the cause of the impaired glucose tolerance (figs. S3, D to F, and S4A). Despite the fact that we have treated male rats with a higher dose of ethanol (3.45 g/kg), the effect of binge drinking on glucose tolerance was more pronounced in females (Fig. 1B and fig. S3, A and B), corroborating clinical evidence indicating that females are more sensitive to the detrimental metabolic effects of binge drinking than males (1). Because oral administration of ethanol through gavage requires restraining of the animals, which can dislodge the intravascular and/or the intracerebroventricular catheters, we used intraperitoneal injections to administer ethanol in all subsequent experiments.

Binge drinking induces persistent hepatic and adipose tissue insulin resistance

To probe the effects of ethanol treatment on insulin action further, we performed hyperinsulinemic euglycemic pancreatic clamp studies in conscious female rats subjected to the same binge drinking paradigm as illustrated in Fig. 1A. This clamp protocol allows insulin concentrations to be raised to a defined value while maintaining euglycemia and is considered the gold standard for assessing insulin action. We assessed glucose and glycerol fluxes with a tracer dilution technique using [^3H]glucose and [^2H -5]glycerol during the clamps. Throughout the study, there were no differences in body weight between groups (Table 1). Blood alcohol concentrations were undetectable during the steady-state phase of the clamp when hGP, glucose utilization, and glycerol appearance were determined (fig. S1A). Serum alanine aminotransferase (ALT) and aspartate aminotransferase (AST) concentrations were not different between groups before the pancreatic clamp was started

(fig. S8). Under baseline conditions, before the hyperinsulinemic clamp was initiated, plasma glucose concentrations were significantly higher in the ethanol-treated group, although hGP values were not different (Fig. 1, C and F). During the hyperinsulinemic clamp ($3 \text{ mU kg}^{-1} \text{ min}^{-1}$), which was initiated after a 2-hour tracer equilibration period, glycemia was well matched between groups (Fig. 1C) and plasma insulin levels were equally raised (Fig. 1E). Plasma lipid levels were not different between groups during the clamp (tables S1 and S2). The glucose infusion rate (GIR) required to maintain euglycemia was significantly lower ($P = 0.002$) in the ethanol group, consistent with insulin resistance (Fig. 1D). Binge drinking impaired the ability of insulin to suppress hGP during the clamp (91% compared to 63%, $P < 0.01$) (Fig. 1G), whereas peripheral glucose disposal was not altered (Fig. 1H), demonstrating that impaired hepatic insulin action mostly accounted for the systemic insulin resistance with regard to glucose metabolism. To test whether binge drinking impairs hepatic insulin signaling, which could account for the functional hepatic insulin resistance, we assessed insulin signaling in the liver harvested at the end of the hyperinsulinemic clamp. Insulin receptor protein expression and the phosphorylation state of the downstream signaling molecule AKT at Thr³⁰⁸ and Ser⁴⁷³ were not reduced in the ethanol-exposed rats, suggesting that insulin signaling during the clamp was not different (fig. S5A). Systemic hyperinsulinemia decreased the rate of appearance (Ra) of glycerol, which provides an estimate of lipolysis by WAT, but failed to do so in rats after binge drinking (Fig. 1I), indicating impaired insulin action in adipose tissue. Because increased lipolytic flux (glycerol and free fatty acids) from WAT to the liver can drive hepatic gluconeogenesis, it is likely that the excess lipolysis contributes to the hepatic insulin resistance in ethanol-treated rats.

To investigate whether insulin resistance persists after cessation of binge drinking, we repeated the studies described above 30 hours after ethanol administration. During the baseline period of the clamp (0 to 120 min), hGP was not different between groups (fig. S6A). Hyperinsulinemia did not suppress hGP in rats that had been given ethanol to the same degree than it did in control rats (suppression of hGP, 96% versus 74%; $P = 0.044$) (fig. S6B), demonstrating that binge drinking leads to a long-lasting metabolic impairment (fig. S6).

Binge drinking impairs hypothalamic insulin action

Insulin regulates systemic glucose and lipid fluxes, in part through signaling in the hypothalamus (10, 11). Ethanol is a well-known neurotoxin (36), and thus, we speculated that the metabolic effects of alcohol may, in part, be due to impaired hypothalamic control of nutrient fluxes in addition to toxic end-organ effects of ethanol on liver and adipose tissue. Because systemic hyperinsulinemia induces insulin signaling in both the brain and the liver, one cannot distinguish peripheral from central effects of insulin during a systemic hyperinsulinemic clamp. One way of probing hypothalamic insulin action in rodents, defined as the ability of insulin signaling in the mediobasal hypothalamus (MBH) to suppress hGP and WAT lipolysis, is to infuse insulin directly into the MBH while maintaining circulating insulin at basal levels, mimicking the fasting state. This induces insulin signaling selectively in the MBH without the direct effects of insulin on the liver and adipose tissue. MBH infusions can be performed during a euglycemic pancreatic clamp to allow assessment of glucose and lipid fluxes with tracer techniques, as outlined above. Because hepatic insulin action was impaired by binge drinking even though hepatic insulin signaling was unaltered at the end of a hyperinsulinemic clamp (fig. S5A), we tested whether this effect might be a result of altered insulin action in the hypothalamus. All published studies that have examined hypothalamic insulin action with the approach described above have been performed in male rodents. Because there are gender differences in brain insulin action in mice and humans (22, 37), we first tested whether insulin delivered

directly to the MBH suppressed hGP and lipolysis in female SD rats as we and others have reported for male SD rats (10, 11). To this end, rats were first fitted with stereotactic cannulae in the MBH and, after 1 week of recovery, implanted with vascular catheters in the carotid artery and the jugular vein. After full recovery, conscious rats were infused with either insulin (2 μ U) or vehicle into the MBH for 6 hours and subjected to euglycemic pancreatic clamps (Fig. 2A). Plasma insulin concentrations were maintained at basal values during the clamp (0.8 mU kg⁻¹ min⁻¹). Blood insulin and glucose concentrations were comparable during baseline and clamped conditions between groups (Fig. 2, B and D). Plasma lipid levels were not different between groups during the clamp (tables S1 and S2). Average GIR to maintain euglycemia was higher in the MBH insulin-infused group compared to the artificial cerebrospinal fluid (aCSF)-infused group 150 min into the clamp (Fig. 2C), but this effect was not significant at later times. MBH insulin suppressed hGP by 32% compared to only 13% in MBH vehicle-infused rats ($P = 0.047$) (Fig. 2, E and F). Glucose disposal during the clamp was not different between groups (Fig. 2G). Ra glycerol, a measure of lipolysis, was decreased by more than 80% in rats infused with MBH insulin compared to vehicle-infused controls during baseline and clamp period (Fig. 2H). These results establish that in female SD rats hypothalamic insulin restrains hGP and lipolysis to a similar degree as in males (10, 11).

Next, we asked whether binge drinking impaired the ability of hypothalamic insulin to suppress hGP and lipolysis. Female SD rats were again injected daily with alcohol for 3 days and then given either vehicle or insulin infusions into the MBH, and were subjected to basal euglycemic pancreatic clamps (Fig. 3A). Glucose (Fig. 3B) and insulin concentrations (0.44 versus 0.45 μ g/liter, $P = 0.95$, and 0.41 versus 0.39 μ g/liter, $P = 0.79$, respectively) (Fig. 3D) did not differ during both baseline and clamped conditions between groups. Plasma lipid levels during the clamp are shown in tables S1 and S2. Average GIR required to maintain euglycemia during the clamp was not different between groups ($P = 0.246$) (Fig. 3C). Binge drinking eliminated the ability of MBH-infused insulin to suppress hGP [25% in vehicle-treated compared to 21% in insulin-infused animals ($P = 0.847$)] (Fig. 3, E and F), whereas glucose disposal remained unaffected (Fig. 3G). Notably, MBH-infused insulin also failed to suppress Ra glycerol (Fig. 3H). Unrestrained lipolytic flux from adipose tissue is likely to contribute to hepatic insulin resistance by driving gluconeogenesis (38). Thus, these data demonstrate that binge drinking markedly impairs the ability of the hypothalamus to respond to insulin, which likely contributes to the hepatic and adipose tissue insulin resistance that we observed in ethanol-treated animals.

Binge drinking impairs MBH and adipose tissue insulin signaling

Although hepatic insulin signaling, as assessed by insulin receptor and AKT phosphorylation, was not altered in binged rats at the end of a hyperinsulinemic clamp (fig. S5A) and hepatic insulin action was impaired in ethanol-treated animals, it can be argued that insulin signaling is better assessed after acute insulin exposure to capture the early dynamics and maximal response of insulin signaling. To test this, we injected 100 mU of insulin directly into the portal vein of female rats, the physiological route of insulin delivery to the liver. Again, binge drinking did not alter insulin receptor protein expression in the liver. The insulin injection induced marked phosphorylation of the insulin receptor and AKT (Ser⁴⁷³ and Thr³⁰⁸) in both groups within 15 min, which was not impaired by ethanol exposure (Fig. 4A). These findings suggest that binge drinking does not impair hepatic insulin action by disrupting insulin signaling in the liver but rather through extrahepatic mechanisms. In contrast, insulin signaling in WAT was decreased (Fig. 4B), possibly contributing to the adipose tissue insulin resistance that we noted and that has also been described in a model of chronic alcohol exposure (39). Next, we determined whether binge drinking altered insulin signaling in the hypothalamus, which could be a cause of the

impaired hypothalamic insulin action. Eight hours after the last ethanol injection, we infused a bolus of 1 mU of insulin or vehicle intraparenchymally into the MBH. Twenty minutes later, animals were sacrificed, and the MBH was dissected for further analysis as described (11). Binge drinking did not alter the total amount of insulin receptor in the MBH (Fig. 4C). As expected, MBH insulin infusion induced autophosphorylation of the insulin receptor in the control group. However, binge drinking markedly blunted insulin-induced autophosphorylation of the insulin receptor in the brain (Fig. 4C), suggesting that impaired hypothalamic insulin action is due to decreased insulin signaling in the MBH.

Binge drinking induces elevated PTP1B levels and inflammation in the hypothalamus

Potential causes for the insulin signaling defect are induction of phosphatases (40) and inflammation (41–43), both molecular pathways that can inhibit insulin signaling. To begin to explore these mechanisms, we assessed the expression of phosphatases and proinflammatory cytokines in the MBH. We found that binge drinking increased the expression of several proinflammatory cytokine genes such as interleukin-6 (*IL-6*) and tumor necrosis factor- α (*TNFA*), which are induced by the inhibitor of κ B/nuclear factor κ light chain enhancer of activated B cells (IKK β /NF κ B) pathway. We assessed three tyrosine phosphatase genes: *PTPNI* (PTP1B), *PTPRA* (receptor-type tyrosine-protein phosphatase α), and *PTPRF* (receptor-type tyrosine-protein phosphatase F). Of these, only PTP1B was significantly increased by binge drinking (Fig. 4D). Our data suggest that binge drinking may compromise hypothalamic insulin signaling and induce inflammation in the MBH, potentially through the regulation of PTP1B.

Inhibition of PTP1B restores glucose tolerance after binge drinking

To further probe the role of PTP1B and the IKK β /NF κ B pathway within the central nervous system in binge drinking-induced insulin resistance, we continuously infused inhibitors of either PTP1B or IKK β into the lateral ventricle using osmotic minipumps. Two days after minipump implantation, once the intracerebroventricular infusion rate was stable, we exposed the rats to ethanol according to the binge drinking paradigm (Fig. 1A) and performed GTTs 8 to 10 hours, 30 hours, and 54 hours after the last ethanol dose (Fig. 5, A to C). To inhibit PTP1B, we used the small-molecule inhibitor CPT-157633 (0.2 μ g/day), and for IKK β , we used the compound PS1145 (2 μ g/day) (44, 45). As we had previously found, binge drinking impaired glucose tolerance, and this effect persisted up to 54 hours after the last ethanol dose (Fig. 5C). Pharmacological inhibition of central PTP1B almost completely prevented glucose intolerance in the ethanol-exposed rats, whereas the IKK β inhibitor PS1145 initially worsened glucose tolerance in this group after 8 to 10 hours. Only at later time points (TPs) did the IKK β inhibitor moderately improve glucose homeostasis (Fig. 5, A to C). Fasting plasma insulin values were increased by binge drinking 8 to 10 hours after the last ethanol dose, which was alleviated by PTP1B inhibition, although at later TPs, neither ethanol exposure nor PTP1B inhibition altered fasting insulin levels (fig. S7, A to C). Intracerebroventricular infusion of either CPT-157633 or PS1145 alleviated the hypothalamic inflammation induced by binge drinking (Fig. 5D), yet only PTP1B inhibition restored glucose tolerance. These results demonstrate that binge drinking may induce systemic insulin resistance by increasing hypothalamic PTP1B expression and disrupting hypothalamic insulin action, which can be prevented by inhibition of PTP1B in the hypothalamus.

DISCUSSION

Individuals who have a habit of binge drinking exhibit an increased risk of developing the metabolic syndrome (1, 3, 4). Here, we demonstrate in a rat model that binge drinking induces insulin resistance in female and male rats, independent of alterations in caloric

intake. Further, disrupted insulin action in hepatic and adipose tissue is a secondary result of impaired hypothalamic insulin action, which can be restored through pharmacological inhibition of hypothalamic PTP1B. Thus, alcohol can impair hepatic carbohydrate metabolism and increase fatty acid flux to the liver indirectly through its effects on the central nervous system, specifically the hypothalamus.

Adipose tissue and liver are both organs in which neuroendocrine regulation via the autonomic nervous system is important, unlike muscle where hypothalamic insulin action does not contribute to, for example, the regulation of glucose uptake. Our studies point to two mechanisms that contribute to the hepatic insulin resistance induced by binge drinking. First, impaired insulin action in adipose tissue increases free fatty acid and glycerol flux to the liver, which in turn worsens hepatic insulin action by increasing the supply of gluconeogenic substrates (46). Second, hypothalamic insulin action, defined as the ability of centrally infused insulin to suppress hGP and WAT lipolysis, and hypothalamic insulin signaling, measured by phosphorylation of insulin receptor and AKT, are markedly reduced.

The notion that binge drinking causes insulin resistance by impairing autonomic control of liver and WAT metabolism is supported by the clinical observation that chronic alcohol consumption is associated with reduced heart rate variability, at manifestation of autonomic dysfunction (47). Further, acute alcohol intoxication increases sympathetic nerve activity (47, 48). Unopposed sympathetic drive is believed to be an important cause of the metabolic dysfunction in obesity and type 2 diabetes (49). We have previously demonstrated that brain insulin dampens sympathetic outflow to WAT, resulting in a suppression of lipolysis (11), whereas hypothalamic insulin resistance exacerbates lipolysis. Together, these results indicate that binge drinking likely leads to autonomic dysfunction, in part by attenuating brain insulin action, which disrupts glucose and lipid flux in liver and WAT.

The biological relevance of impaired hypothalamic insulin action is highlighted by our finding that the inhibition of PTP1B, an inhibitor of insulin signaling, prevents the impairment in systemic carbohydrate metabolism. Thus, these studies provide proof of principle that binge drinking–induced impairment of insulin action is primarily a consequence of decreased insulin signaling in the MBH. After drinking, hepatic insulin signaling was not altered after acute insulin treatment or after prolonged physiological hyperinsulinemia induced by hyperinsulinemic clamping. Although these studies support the notion that impaired hepatic insulin action after binge drinking is caused by deficient hypothalamic insulin action and not reduced hepatic insulin signaling, insulin dose-response studies may unveil more subtle defects in hepatic insulin signaling. Acute alcohol exposure inhibits autophosphorylation of the insulin receptor (50). In our experiments, however, this does not explain the ethanol-induced systemic insulin resistance that we observed, because alcohol was no longer present when we assessed both insulin action and signaling (50). Notably, the major toxic metabolite of alcohol, acetaldehyde, does not inhibit insulin signaling in neuronal cells (51). Finally, we demonstrate that selective inhibition of PTP1B only in the hypothalamus is sufficient to prevent the systemic insulin resistance induced by binge drinking. Precisely how alcohol increases the expression of PTP1B in the MBH remains to be determined. Aging and overnutrition, both common causes of systemic insulin resistance, also increase hypothalamic PTP1B expression (26, 52, 53).

Binge drinking also increased the expression of proinflammatory cytokines such as IL-6 and TNF- α within the MBH, a manifestation of hypothalamic inflammation. Hypothalamic inflammation can reduce insulin signaling in the hypothalamus and is an important cause of the disrupted neuroendocrine control of metabolism in obesity that results in systemic insulin resistance (40–43, 54). Nevertheless, in our model of binge drinking–induced glucose intolerance and insulin resistance, inhibition of the IKK β /NF κ B pathway was not

sufficient to restore glucose homeostasis, although it improved glucose tolerance moderately on the second and third day after the last ethanol dose. Surprisingly, at an earlier TP, 8 hours after the last dose of ethanol, inhibition of the NF κ B pathway worsened glucose tolerance, which suggests that hypothalamic inflammation may initially be adaptive and only later becomes maladaptive resulting in metabolic impairment. Our results also suggest that inflammation per se may not be the primary mediator of ethanol-induced hypothalamic insulin resistance because both the IKK β /NF κ B and PTP1B inhibitor reduce hypothalamic inflammation, yet only PTP1B inhibition restores glucose tolerance. Whole-body PTP1B knockout mice are protected from aging-induced insulin resistance and WAT inflammation, and our results support a role of hypothalamic PTP1B in this protective phenotype (55).

There are certain limitations to our study. We administered ethanol through intraperitoneal injections for experimental reasons, which is not the physiological route of alcohol administration. Nevertheless, we did observe similar effects on glucose tolerance when ethanol was administered through oral gavage, indicating that the route of administration is not that critical in ethanol-induced insulin resistance in rats.

In summary, our studies demonstrate that ethanol impairs glucose and lipid metabolism in rats through neurotoxic effects in the hypothalamus. The resulting insulin resistance persists days after all ethanol has been metabolized. If these results apply to humans, binge drinking is not only an epidemiological risk factor but also a direct cause of insulin resistance that sets the stage for the metabolic syndrome and type 2 diabetes.

MATERIALS AND METHODS

Experimental design

After surgery and recovery period, rats were randomized to each individual treatment group. All GTTs were performed blinded and repeated twice. Clamp studies were performed once.

Animals

Animal protocols were approved by the Icahn School of Medicine at Mount Sinai Institutional Animal Care and Use Committee. Twelve to 14-week-old female and male SD rats (Charles River Breeding Laboratories) were housed under controlled temperature, humidity, and light cycles (12:12 hours). Standard chow diet (Rodent Diet 5001, LabDiet) and water were available ad libitum. Two weeks before the clamp study, rats participating in central infusion studies were stereotactically implanted with a guide cannula targeting the MBH as described by Scherer *et al.* (11). One week later, carotid and jugular catheters were implanted for blood sampling and infusion. Rats were allowed to recover for 8 days and required to return to within 10% of their presurgical body weight (Table 1). Rats that were part of the 3-mU clamp protocol without central infusions were only implanted with vascular catheters.

Ethanol feeding

Female SD rats were injected intraperitoneally or orally gavaged daily with ethanol (3 g/kg) in a 20% (v/v) ethanol/saline solution on three consecutive days always between 7 and 8 a.m. Male rats were injected daily with ethanol (3.45 g/kg, intraperitoneally) in a 20% (v/v) ethanol/saline solution on three consecutive days always between 7 and 8 a.m. Rats in the control group were injected with an isocaloric glucose/saline solution for all experiments except the GTT in Fig. 1B, where the control group was injected with saline. Intraperitoneal injections are widely used in rodent models, and many studies have shown that oral and intraperitoneal administration yield similar results for several biological readouts (34, 35, 56, 57). Intraperitoneal administration also avoids the first-pass gastric metabolism of

ethanol, which can vary depending on the nutritional state of the animal and adds an additional variable. After intraperitoneal injection, ethanol is absorbed by the visceral peritoneum and intraperitoneal organs that drain into the portal venous system and thereby the liver. To ensure similar food intake (58), rats were pair-fed throughout the study (Table 1 and fig. S7D). Food intake was measured by manually weighing food pellets for the ethanol-treated group, and the glucose-injected group was fed the same amount of food. Experiments were performed either 8 to 10, 30, or 54 hours after the third dose of ethanol as indicated.

Glucose tolerance test

Fourteen-week-old female or male SD rats were treated with ethanol as above to simulate binge drinking. After the last dose, rats were fasted for 8 to 10 hours until alcohol had been metabolized. Rats were then injected intraperitoneally with glucose (2 or 3 g/kg) (Fig. 5 and fig. S3, A to C) in a 20% glucose/saline solution. Blood glucose was measured with an AlphaTRAK glucometer (Abbott Laboratories). Tail vein samples were taken at 0, 7.5, 15, 30, 60, 90, and 120 min after glucose injection to measure glucose and at 0, 30, and 90 min to measure insulin levels.

Hepatic insulin signaling studies

Fourteen-week-old female SD rats were treated with ethanol to simulate binge drinking. After the last dose, rats were fasted and experiments were started when alcohol had been metabolized (8 to 10 hours after injection). Rats were anesthetized with ketamine-xylazine, a midline incision was performed, and viscera were exposed. Using a 26-gauge needle, we injected 100 mU of insulin (Humulin R, Lilly) in 100 μ l of saline into the portal vein, and 3 min after injection, we sacrificed the animals by decapitation. The liver was snap-frozen in liquid nitrogen and kept at -80°C for further analysis.

Brain signaling studies

Fourteen-week-old female SD rats were implanted with cannulae targeting the MBH as described above, and 1 week later, experiments were performed. After the last dose of ethanol, rats were fasted and experiments were started when alcohol had been metabolized (8 to 10 hours after injection). Conscious, nonrestrained rats were given a dose of either 1 μ l of aCSF (vehicle) or 1 mU of insulin in 1 μ l of aCSF (Humulin R, Lilly), intraparenchymally administered over 1 min into each side of the MBH. Twenty minutes later, animals were anesthetized with isoflurane and decapitated, and the MBH was dissected, snap-frozen in liquid nitrogen, and kept at -80°C for further analysis.

PTP1B and IKK β inhibitor experiments

Fourteen-week-old female SD rats were implanted with osmotic minipumps (model 1004, Durect Corporation) and Brain Infusion Kit 2. Pumps were filled with either PS1145 (2 μ g/day) (Sigma-Aldrich) or a small-molecule inhibitor of PTP1B (CPT-157633) (0.2 μ g/day) (Ceptyr Inc.; US Patent US 7,504,389B2) (45). CPT-157633 (molecular weight, 465) was developed as an active site-directed inhibitor. It is a difluoro-phosphonomethyl phenylalanine derivative, which is a non-hydrolyzable phosphotyrosine mimetic that is resistant to PTP action. We chose the dose of the inhibitors based on work that was done with compounds of similar kinetics. We also found in previous experiments that higher doses decreased food intake, and therefore chose the above-mentioned doses. PS1145 was dissolved in 7.75% β -cyclodextrin and aCSF, and CPT-157633 was dissolved in aCSF. The pumps were filled shortly before implantation, and a pump rate of 0.11 μ l/hour was stable after 48 hours of priming in the animal. We cannulated the right lateral ventricle 1.9 mm posterior from bregma, 2.5 mm right lateral from the sagittal suture, and 5 mm below the surface of the skull. Placement was controlled and verified by infusing food dye. Forty-eight

hours after pump implantation, female rats were treated with ethanol as described above, and GTTs were performed 8 to 10, 30, and 54 hours after the last dose of ethanol. After the last GTT, animals were anesthetized with isoflurane and decapitated, and cannula placement was confirmed by infusing food dye. For gene expression analysis in Fig. 5D, female rats were implanted with minipumps as mentioned above and subjected to our binge drinking model, and tissue was harvested 10 hours after the last ethanol dose for further analysis.

MBH cannulation

Experiments were performed in adult rats (12 to 14 weeks old), and ketamine-xylazine was used for all surgical interventions. Two weeks before the clamp study, rats participating in central infusion studies were stereotactically implanted with a 26-gauge dual guide cannula (Plastics One) in the MBH, 3.3 mm posterior from bregma, 0.4 mm bilateral from midline, and 9.6 mm below the surface of the skull. Coordinates were according to Paxinos Rat Brain Atlas (59). Guide cannulae were blocked with dummy cannulae (Plastics One) until the day of the experiment. Food dye was regularly infused immediately before removing the brain to confirm correct anatomical placement of the cannulae. One week later, carotid and jugular catheters were implanted for blood sampling and infusion. Rats were allowed to recover for 8 days and required to weigh within 10% of their presurgical body weight. Rats that were part of the 3-mU clamp protocol without central infusions were only implanted with catheters as described above.

Rat pancreatic clamp studies

Rat clamp experiments were performed on conscious, nonrestrained, pair-fed female SD rats. During the 360-min study protocol, rats were kept in individual plastic cages with bedding. At the start, MBH infusion cannulae were inserted into the guide cannulae. An MBH (0.18 $\mu\text{l}/\text{hour}$ per side) infusion with either vehicle (aCSF) (Harvard Apparatus) or human insulin (2 μU) (Humulin R, Lilly) was started at TP -120 min and maintained for the entire 6-hour study. At TP 0, a 120-min tracer equilibration period was started in which a 20- μCi bolus of [$3\text{-}^3\text{H}$]glucose (radiochemical concentration >97%) (PerkinElmer) and a 40- μmol bolus of [$2\text{-}^3\text{H}$]glycerol (99 atomic % excess) (Cambridge Isotope Laboratories Inc.) followed by infusions of [$3\text{-}^3\text{H}$]glucose (0.5 $\mu\text{Ci}/\text{min}$) and [$2\text{-}^3\text{H}$]glycerol (1 $\mu\text{mol}/\text{min}$) were started. For the last 30 min of the tracer equilibration period, arterial blood samples were collected every 10 min to determine baseline GP and rate of appearance (Ra) of glycerol using tracer dilution methodology. At TP 120 min, the pancreatic clamp was started with a primed-continuous infusion of human insulin (bolus of 14.2 or 53.2 mU kg^{-1} followed by an infusion of 0.8 or 3 $\text{mU kg}^{-1} \text{min}^{-1}$) (Humulin R, Lilly) and a simultaneous infusion of somatostatin (3 $\mu\text{g kg}^{-1} \text{min}^{-1}$). The tracer infusions were continued at the aforementioned rates. Euglycemia (~110 to 130 mg/dl) was maintained during the clamp by measuring blood glucose every 10 min starting at TP 120 min and infusing 25% glucose as needed. Arterial blood samples were obtained every 10 min for the last hour of the experiment (TP = 180 to 240 min) to calculate GP, the rate of glucose disposal, and the Ra glycerol under clamped conditions. Pancreatic clamps that did not require brain infusions were started with a tracer equilibration period, and the protocol was shortened to 240 min as depicted in Fig. 1A.

Glucose tracer analysis

To measure plasma [$3\text{-}^3\text{H}$]glucose radioactivity, samples were deproteinated with barium hydroxide and zinc sulfate. After centrifugation, the supernatant was dried overnight to eliminate tritiated water. Glucose was then redissolved in water, and radioactivity was measured with Ultima Gold in a MicroBeta TriLux (PerkinElmer) liquid scintillation counter. Under preclamp steady-state conditions, the endogenous GP equals the glucose turnover rate, which was determined from the ratio of the [$3\text{-}^3\text{H}$]glucose tracer infusion rate

and the specific activity of plasma glucose. During the clamp period, endogenous GP was calculated by subtracting the GIR from the glucose turnover rate, which in a steady state equals the rate of glucose disposal and glucose uptake in muscle, liver, and WAT.

Glycerol fluxes

Ra glycerol (in $\mu\text{mol kg}^{-1} \text{min}^{-1}$) was calculated by the equation $Ra = (\text{ENRinf}/\text{ENRpl} - 1) \times R$, where ENRinf is the fractional isotopic enrichment of the infused glycerol in atomic percent excess and ENRpl is the enrichment in the plasma sample. R is the rate of isotope infusion in $\mu\text{mol kg}^{-1} \text{min}^{-1}$ (60). The ^2H labeling of plasma glycerol was determined with an Agilent 5973N-MSD equipped with an Agilent 6890GC system and an ADB-17MS capillary column (30 m \times 0.25 mm \times 0.25 m) and as follows: 20 μl of plasma was deproteinated with 200 μl of methanol by centrifugation. The fluid fraction was dried and reacted with 50 μl of pyridine and 50 μl of acetic anhydride for 20 min. Isotope enrichment was determined by gas chromatography–mass spectrometry. Ions of 236 to 241 mass-to-charge ratios were monitored.

Western blot analyses

Liver, WAT, or hypothalamus was homogenized in 20 mM Mops, 2 mM EGTA, 5 mM EDTA, 30 mM sodium fluoride, 40 mM β -glycerophosphate, 10 mM sodium pyrophosphate, 2 mM sodium orthovanadate, 0.5% NP-40, and complete protease inhibitor cocktail (Roche) and centrifuged at 13,000g for 20 min at 4 or 0°C. Protein concentration in the supernatant was measured with a BCA protein quantification kit (Thermo Scientific). Samples of 10 to 20 μg of total protein extract were separated on 4 to 12% NuPAGE gels (Invitrogen) and blotted onto Immobilon-FL PVDF (Millipore). Membranes were blocked at room temperature for 1 hour in Odyssey LI-COR Blocking Buffer (1:1; LI-COR), diluted in tris-buffered saline (TBS), and incubated in primary antibodies in 1:1 Blocking Buffer/TBS-T overnight at 4°C. We used primary antibodies against phospho-AKT (Thr³⁰⁸ and Ser⁴⁷³), phospho-insulin receptor β (all Cell Signaling Technology Inc.), β -actin (Sigma-Aldrich Co.), and insulin receptor β (Santa Cruz Biotechnology). After three consecutive 5-min washes in TBS-T (0.1%), blots were incubated with DyLight 800–conjugated goat anti-rabbit immunoglobulin G (IgG) and DyLight 680–conjugated goat anti-mouse IgG (both Thermo Scientific) for 1 hour at room temperature in blocking buffer containing 0.1% TBS-T and 0.1% SDS. After three washes in TBS-T and a final wash in TBS, the blots were scanned on a Odyssey scanner (LI-COR) and quantified with Odyssey 3.0 software on the basis of direct fluorescence values.

RNA extractions and qRT-PCR

Total RNA was obtained from frozen MBH with the RNeasy Lipid Tissue Kit (Qiagen). After treatment with DNase I (Invitrogen), purified total RNA was used for first-strand complementary DNA synthesis with SuperScript III (Invitrogen). We ran qRT-PCR with SYBR GreenER qPCR SuperMix (Invitrogen) on a 7900HT sequence detection system (Applied Biosystems). The forward and reverse customized primers (Invitrogen) are listed below. Data were analyzed with the comparative C_t method (61).

The sequences of qRT-PCR primers were as follows: *IL-6*, 5'-AGTTGCCTTCTTGGGACTGA-3' (forward) and 5'-ACAGTGCATCATCGCTGTTTC-3' (reverse); *TNFA*, 5'-ACGATGCTCAGAAACACACG-3' (forward) and 5'-CAGTCTGGGAAGCTCTGAGG-3' (reverse); *PTPN1*, 5'-CGGAACAGGTACCGAGATGT-3' (forward) and 5'-CCACACCATCTCCCAGAAGT-3' (reverse); *IL-1B*, 5'-AAAATGCCTCGTGCTGTCT-3' (forward) and 5'-GGGATTTTGTGCTTGCTTGT-3' (reverse); *SOCS3*, 5'-TTCTTTACCACCGACGGAAC-3' (forward) and 5'-

GTAGCCACGTTGGAGGAGAG-3' (reverse); *PTPRF*, 5'-TCAAGACACAGCAGGGAGTG-3' (forward) and 5'-GCTTCAGGTCCTCCAGAGTG-3' (reverse); *PTPRA*, 5'-AGGCCCTTCTGGAGCATTAT-3' (forward) and 5'-GTTTCCCGTACGCATCTTGT-3' (reverse); *GAPDH*, 5'-AGACAGCCGCATCTTCTTGT-3' (forward) and 5'-CTTGCCGTGGGTAGAGTCAT-3' (reverse).

Lipid analysis

Plasma triglycerides (TGs) were measured with a TG kit from Sigma (Sigma-Aldrich Inc.) according to the manufacturer's protocol. Plasma nonesterified fatty acid (NEFA) levels were determined with a NEFA kit from Wako Chemicals USA Inc. following the manufacturer's protocol.

Insulin enzyme-linked immunosorbent assay

Insulin levels were determined with Mercodia Insulin ELISA according to the manufacturer's protocol. Data were analyzed by performing cubic spline regression with GraphPad Prism (GraphPad Software).

Alcohol assay

Alcohol levels were measured in serum right after collection with a Pointe Scientific alcohol reagent kit according to the manufacturer's protocol.

Statistics

All values are presented as means \pm SEM unless noted otherwise. Comparisons between groups were made with unpaired two-tailed Student's *t* tests. Repeated measurements within the same group were compared by two-way ANOVA followed by Bonferroni posttest (insulin levels, hGP, and Ra glycerol during baseline and insulin-clamped conditions) (GraphPad Prism, GraphPad Software). Differences were considered statistically significant at $P < 0.05$.

Supplementary Material

Refer to Web version on PubMed Central for supplementary material.

Acknowledgments

We thank M. H. Tschoep and C.-X. Yi for helpful discussions.

Funding: This work was supported by NIH grants DK074873, DK083568, and DK082724 to C.B., by a European Foundation for the Study of Diabetes grant to C.L., and by U24 DK76169 to Mouse Metabolic Phenotyping Center, Case Western Reserve University.

REFERENCES AND NOTES

1. Carlsson S, Hammar N, Grill V, Kaprio J. Alcohol consumption and the incidence of type 2 diabetes: A 20-year follow-up of the Finnish twin cohort study. *Diabetes Care*. 2003; 26:2785–2790. [PubMed: 14514580]
2. Fan AZ, Russell M, Naimi T, Li Y, Liao Y, Jiles R, Mokdad AH. Patterns of alcohol consumption and the metabolic syndrome. *J. Clin. Endocrinol. Metab*. 2008; 93:3833–3838. [PubMed: 18628524]
3. Lee K. Gender-specific relationships between alcohol drinking patterns and metabolic syndrome: The Korea National Health and Nutrition Examination Survey 2008. *Public Health Nutr*. 2012; 15:1917–1924. [PubMed: 22321717]

4. Cullmann M, Hilding A, Östenson CG. Alcohol consumption and risk of pre-diabetes and type 2 diabetes development in a Swedish population. *Diabet. Med.* 2012; 29:441–452. [PubMed: 21916972]
5. Naimi TS, Brewer RD, Mokdad A, Denny C, Serdula MK, Marks JS. Binge drinking among US adults. *JAMA.* 2003; 289:70–75. [PubMed: 12503979]
6. Mitka M. College binge drinking still on the rise. *JAMA.* 2009; 302:836–837. [PubMed: 19706853]
7. Pincock S. Binge drinking on rise in UK and elsewhere. Government report shows increases in alcohol consumption, cirrhosis, and premature deaths. *Lancet.* 2003; 362:1126–1127. [PubMed: 14552335]
8. Volkow ND, Wang GJ, Baler RD. Reward, dopamine and the control of food intake: Implications for obesity. *Trends Cogn. Sci.* 2011; 15:37–46. [PubMed: 21109477]
9. Mittelman SD, Bergman RN. Inhibition of lipolysis causes suppression of endogenous glucose production independent of changes in insulin. *Am. J. Physiol. Endocrinol. Metab.* 2000; 279:E630–E637. [PubMed: 10950832]
10. Obici S, Zhang BB, Karkanias G, Rossetti L. Hypothalamic insulin signaling is required for inhibition of glucose production. *Nat. Med.* 2002; 8:1376–1382. [PubMed: 12426561]
11. Scherer T, O'Hare J, Diggs-Andrews K, Schweiger M, Cheng B, Lindtner C, Zielinski E, Vempati P, Su K, Dighe S, Milsom T, Puchowicz M, Scheja L, Zechner R, Fisher SJ, Previs SF, Buettner C. Brain insulin controls adipose tissue lipolysis and lipogenesis. *Cell Metab.* 2011; 13:183–194. [PubMed: 21284985]
12. O'Hare JD, Zielinski E, Cheng B, Scherer T, Buettner C. Central endocannabinoid signaling regulates hepatic glucose production and systemic lipolysis. *Diabetes.* 2011; 60:1055–1062. [PubMed: 21447652]
13. Okamoto H, Obici S, Accili D, Rossetti L. Restoration of liver insulin signaling in *Insr* knockout mice fails to normalize hepatic insulin action. *J. Clin. Invest.* 2005; 115:1314–1322. [PubMed: 15864351]
14. Tonks NK. PTP1B: From the sidelines to the front lines! *FEBS Lett.* 2003; 546:140–148. [PubMed: 12829250]
15. Kipfer-Coudreau S, Eberlé D, Sahbatou M, Bonhomme A, Guy-Grand B, Froguel P, Galan P, Basdevant A, Clément K. Single nucleotide polymorphisms of protein tyrosine phosphatase 1B gene are associated with obesity in morbidly obese French subjects. *Diabetologia.* 2004; 47:1278–1284. [PubMed: 15235769]
16. Tsou RC, Bence KK. The genetics of *PTPN1* and obesity: Insights from mouse models of tissue-specific PTP1B deficiency. *J. Obes.* 2012; 2012:926857. [PubMed: 22811891]
17. Elchebly M, Payette P, Michaliszyn E, Cromlish W, Collins S, Loy AL, Normandin D, Cheng A, Himms-Hagen J, Chan CC, Ramachandran C, Gresser MJ, Tremblay ML, Kennedy BP. Increased insulin sensitivity and obesity resistance in mice lacking the protein tyrosine phosphatase-1B gene. *Science.* 1999; 283:1544–1548. [PubMed: 10066179]
18. Delibegovic M, Zimmer D, Kauffman C, Rak K, Hong EG, Cho YR, Kim JK, Kahn BB, Neel BG, Bence KK. Liver-specific deletion of protein-tyrosine phosphatase 1B (PTP1B) improves metabolic syndrome and attenuates diet-induced endoplasmic reticulum stress. *Diabetes.* 2009; 58:590–599. [PubMed: 19074988]
19. Bence KK, Delibegovic M, Xue B, Gorgun CZ, Hotamisligil GS, Neel BG, Kahn BB. Neuronal PTP1B regulates body weight, adiposity and leptin action. *Nat. Med.* 2006; 12:917–924. [PubMed: 16845389]
20. Tschritter O, Preissl H, Hennige AM, Stumvoll M, Porubská K, Frost R, Marx H, Klösel B, Lutzenberger W, Birbaumer N, Häring HU, Fritsche A. The cerebrocortical response to hyperinsulinemia is reduced in overweight humans: A magnetoencephalographic study. *Proc. Natl. Acad. Sci. U.S.A.* 2006; 103:12103–12108. [PubMed: 16877540]
21. Guthoff M, Stingl KT, Tschritter O, Rogic M, Heni M, Stingl K, Hallschmid M, Häring HU, Fritsche A, Preissl H, Hennige AM. The insulin-mediated modulation of visually evoked magnetic fields is reduced in obese subjects. *PLoS One.* 2011; 6:e19482. [PubMed: 21589921]

22. Brüning JC, Gautam D, Burks DJ, Gillette J, Schubert M, Orban PC, Klein R, Krone W, Müller-Wieland D, Kahn CR. Role of brain insulin receptor in control of body weight and reproduction. *Science*. 2000; 289:2122–2125. [PubMed: 11000114]
23. Scherer T, Lindtner C, Zielinski E, O'Hare J, Filatova N, Buettner C. Short term voluntary overfeeding disrupts brain insulin control of adipose tissue lipolysis. *J. Biol. Chem.* 2012; 287:33061–33069. [PubMed: 22810223]
24. Shoelson SE, Lee J, Goldfine AB. Inflammation and insulin resistance. *J. Clin. Invest.* 2006; 116:1793–1801. [PubMed: 16823477]
25. Thaler JP, Schwartz MW. Minireview: Inflammation and obesity pathogenesis: The hypothalamus heats up. *Endocrinology*. 2010; 151:4109–4115. [PubMed: 20573720]
26. Zhang X, Zhang G, Zhang H, Karin M, Bai H, Cai D. Hypothalamic IKK β /NF- κ B and ER stress link overnutrition to energy imbalance and obesity. *Cell*. 2008; 135:61–73. [PubMed: 18854155]
27. Ozcan L, Ergin AS, Lu A, Chung J, Sarkar S, Nie D, Myers MG Jr, Ozcan U. Endoplasmic reticulum stress plays a central role in development of leptin resistance. *Cell Metab.* 2009; 9:35–51. [PubMed: 19117545]
28. Avogaro A, Valerio A, Miola M, Crepaldi C, Pavan P, Tiengo A, del Prato S. Ethanol impairs insulin-mediated glucose uptake by an indirect mechanism. *J. Clin. Endocrinol. Metab.* 1996; 81:2285–2290. [PubMed: 8964865]
29. Boden G, Chen X, DeSantis RA, Kendrick Z. Ethanol inhibits insulin action on lipolysis and on insulin release in elderly men. *Am. J. Physiol.* 1993; 265:E197–E202. [PubMed: 8368288]
30. Onishi Y, Honda M, Ogihara T, Sakoda H, Anai M, Fujishiro M, Ono H, Shojima N, Fukushima Y, Inukai K, Katagiri H, Kikuchi M, Oka Y, Asano T. Ethanol feeding induces insulin resistance with enhanced PI 3-kinase activation. *Biochem. Biophys. Res. Commun.* 2003; 303:788–794. [PubMed: 12670480]
31. Shelmet JJ, Reichard GA, Skutches CL, Hoeldtke RD, Owen OE, Boden G. Ethanol causes acute inhibition of carbohydrate, fat, and protein oxidation and insulin resistance. *J. Clin. Invest.* 1988; 81:1137–1145. [PubMed: 3280601]
32. Avogaro A, Watanabe RM, Dall'Arche A, De Kreutzenberg SV, Tiengo A, Pacini G. Acute alcohol consumption improves insulin action without affecting insulin secretion in type 2 diabetic subjects. *Diabetes Care*. 2004; 27:1369–1374. [PubMed: 15161790]
33. Callaci JJ, Himes R, Lauing K, Roper P. Long-term modulations in the vertebral transcriptome of adolescent-stage rats exposed to binge alcohol. *Alcohol Alcohol.* 2010; 45:332–346. [PubMed: 20554695]
34. Lang CH, Frost RA, Vary TC. Acute alcohol intoxication increases REDD1 in skeletal muscle. *Alcohol. Clin. Exp. Res.* 2008; 32:796–805. [PubMed: 18336631]
35. Knapp DJ, Braun CJ, Duncan GE, Qian Y, Fernandes A, Crews FT, Breese GR. Regional specificity of ethanol and NMDA action in brain revealed with FOS-like immuno-histochemistry and differential routes of drug administration. *Alcohol. Clin. Exp. Res.* 2001; 25:1662–1672. [PubMed: 11707641]
36. Leonard BE. Is ethanol a neurotoxin?: The effects of ethanol on neuronal structure and function. *Alcohol Alcohol.* 1986; 21:325–338. [PubMed: 2434114]
37. Benedict C, Kern W, Schultes B, Born J, Hallschmid M. Differential sensitivity of men and women to anorexigenic and memory-improving effects of intranasal insulin. *J. Clin. Endocrinol. Metab.* 2008; 93:1339–1344. [PubMed: 18230654]
38. Mittelman SD, Bergman RN. Inhibition of lipolysis causes suppression of endogenous glucose production independent of changes in insulin. *Am. J. Physiol. Endocrinol. Metab.* 2000; 279:E630–E637. [PubMed: 10950832]
39. Kang L, Chen X, Sebastian BM, Pratt BT, Bederman IR, Alexander JC, Previs SF, Nagy LE. Chronic ethanol and triglyceride turnover in white adipose tissue in rats: Inhibition of the antilipolytic action of insulin after chronic ethanol contributes to increased triglyceride degradation. *J. Biol. Chem.* 2007; 282:28465–28473. [PubMed: 17686776]
40. Zabolotny JM, Haj FG, Kim YB, Kim HJ, Shulman GI, Kim JK, Neel BG, Kahn BB. Transgenic overexpression of protein-tyrosine phosphatase 1B in muscle causes insulin resistance, but

- overexpression with leukocyte antigen-related phosphatase does not additively impair insulin action. *J. Biol. Chem.* 2004; 279:24844–24851. [PubMed: 15031294]
41. Klover PJ, Zimmers TA, Koniaris LG, Mooney RA. Chronic exposure to interleukin-6 causes hepatic insulin resistance in mice. *Diabetes.* 2003; 52:2784–2789. [PubMed: 14578297]
 42. Senn JJ, Klover PJ, Nowak IA, Zimmers TA, Koniaris LG, Furlanetto RW, Mooney RA. Suppressor of cytokine signaling-3 (SOCS-3), a potential mediator of interleukin-6-dependent insulin resistance in hepatocytes. *J. Biol. Chem.* 2003; 278:13740–13746. [PubMed: 12560330]
 43. Hotamisligil GS, Budavari A, Murray D, Spiegelman BM. Reduced tyrosine kinase activity of the insulin receptor in obesity-diabetes. Central role of tumor necrosis factor- α . *J. Clin. Invest.* 1994; 94:1543–1549. [PubMed: 7523453]
 44. Oh-I S, Thaler JP, Ogimoto K, Wisse BE, Morton GJ, Schwartz MW. Central administration of interleukin-4 exacerbates hypothalamic inflammation and weight gain during high-fat feeding. *Am. J. Physiol. Endocrinol. Metab.* 2010; 299:E47–E53. [PubMed: 20371733]
 45. Mark TB, Blaskovich AT, Baughman T, Little T, Patt W, Qaber M, Schultz LM, Nagula G, Gage JL, Howbert JJ. Protein tyrosine phosphatase inhibitors and methods of use thereof, U.S. Patent. 2009:7504389.
 46. Lewis GF, Vranic M, Harley P, Giacca A. Fatty acids mediate the acute extrahepatic effects of insulin on hepatic glucose production in humans. *Diabetes.* 1997; 46:1111–1119. [PubMed: 9200644]
 47. Quintana DS, McGregor IS, Guastella AJ, Malhi GS, Kemp AH. A meta-analysis on the impact of alcohol dependence on short-term resting-state heart rate variability: Implications for cardiovascular risk. *Alcohol. Clin. Exp. Res.* 2013; 37:E23–E29. [PubMed: 22834996]
 48. van de Borne P, Mark AL, Montano N, Mion D, Somers VK. Effects of alcohol on sympathetic activity, hemodynamics, and chemoreflex sensitivity. *Hypertension.* 1997; 29:1278–1283. [PubMed: 9180629]
 49. Mancia G, Bousquet P, Elghozi JL, Esler M, Grassi G, Julius S, Reid J, Van Zwieten PA. The sympathetic nervous system and the metabolic syndrome. *J. Hypertens.* 2007; 25:909–920. [PubMed: 17414649]
 50. Seiler AE, Henderson A, Rubin R. Ethanol inhibits insulin receptor tyrosine kinase. *Alcohol. Clin. Exp. Res.* 2000; 24:1869–1872. [PubMed: 11141047]
 51. Tong M, Longato L, Nguyen Q-G, Chen WC, Spaisman A, de la Monte SM. Acetaldehyde-mediated neurotoxicity: Relevance to fetal alcohol spectrum disorders. *Oxid. Med. Cell. Long.* 2011; 2011:1–13.
 52. García-San Frutos M, Fernández-Agulló T, Carrascosa JM, Horrillo D, Barrús MT, Oliveros E, Sierra J, Ros M. Involvement of protein tyrosine phosphatases and inflammation in hypothalamic insulin resistance associated with ageing: Effect of caloric restriction. *Mech. Ageing Dev.* 2012; 133:489–497. [PubMed: 22733037]
 53. White CL, Whittington A, Barnes MJ, Wang Z, Bray GA, Morrison CD. HF diets increase hypothalamic PTP1B and induce leptin resistance through both leptin-dependent and -independent mechanisms. *Am. J. Physiol. Endocrinol. Metab.* 2009; 296:E291–E299. [PubMed: 19017730]
 54. Schenk S, Saberi M, Olefsky JM. Insulin sensitivity: Modulation by nutrients and inflammation. *J. Clin. Invest.* 2008; 118:2992–3002. [PubMed: 18769626]
 55. González-Rodríguez A, Más-Gutierrez JA, Mirasierra M, Fernandez-Pérez A, Lee YJ, Ko HJ, Kim JK, Romanos E, Carrascosa JM, Ros M, Vallejo M, Rondinone CM, Valverde AM. Essential role of protein tyrosine phosphatase 1B in obesity-induced inflammation and peripheral insulin resistance during aging. *Aging Cell.* 2012; 11:284–296. [PubMed: 22221695]
 56. Smith T, DeMaster EG, Furne JK, Springfield J, Levitt MD. First-pass gastric mucosal metabolism of ethanol is negligible in the rat. *J. Clin. Invest.* 1992; 89:1801–1806. [PubMed: 1601990]
 57. Ogilvie K, Lee S, Rivier C. Effect of three different modes of alcohol administration on the activity of the rat hypothalamic-pituitary-adrenal axis. *Alcohol. Clin. Exp. Res.* 1997; 21:467–476. [PubMed: 9161607]
 58. Gadeholt G, Stowell A, Mørland J. Acute ethanol intoxication decreases subsequent food intake and changes hepatic microsomal enzyme activities similarly to fasting. *Acta Pharmacol. Toxicol.* 1983; 53:417–420.

59. Paxinos, G. *The Rat Brain in Stereotaxic Coordinates*. ed. 6. Waltham, MA: Academic Press; 2009.
60. Stumvoll M, Jacob S. Multiple sites of insulin resistance: Muscle, liver and adipose tissue. *Exp. Clin. Endocrinol. Diabetes*. 1999; 107:107–110. [PubMed: 10320049]
61. Schmittgen TD, Livak KJ. Analyzing real-time PCR data by the comparative C_T method. *Nat. Protoc*. 2008; 3:1101–1108. [PubMed: 18546601]
62. Lindtner C, Scherer T, Zielinski E, Filatova N, Fasshauer M, Tonks NK, Puchowicz M, Buettner C. Binge drinking induces whole-body insulin resistance by impairing hypothalamic insulin action. *Sci. Transl. Med*. 2013; 5 170ra14.

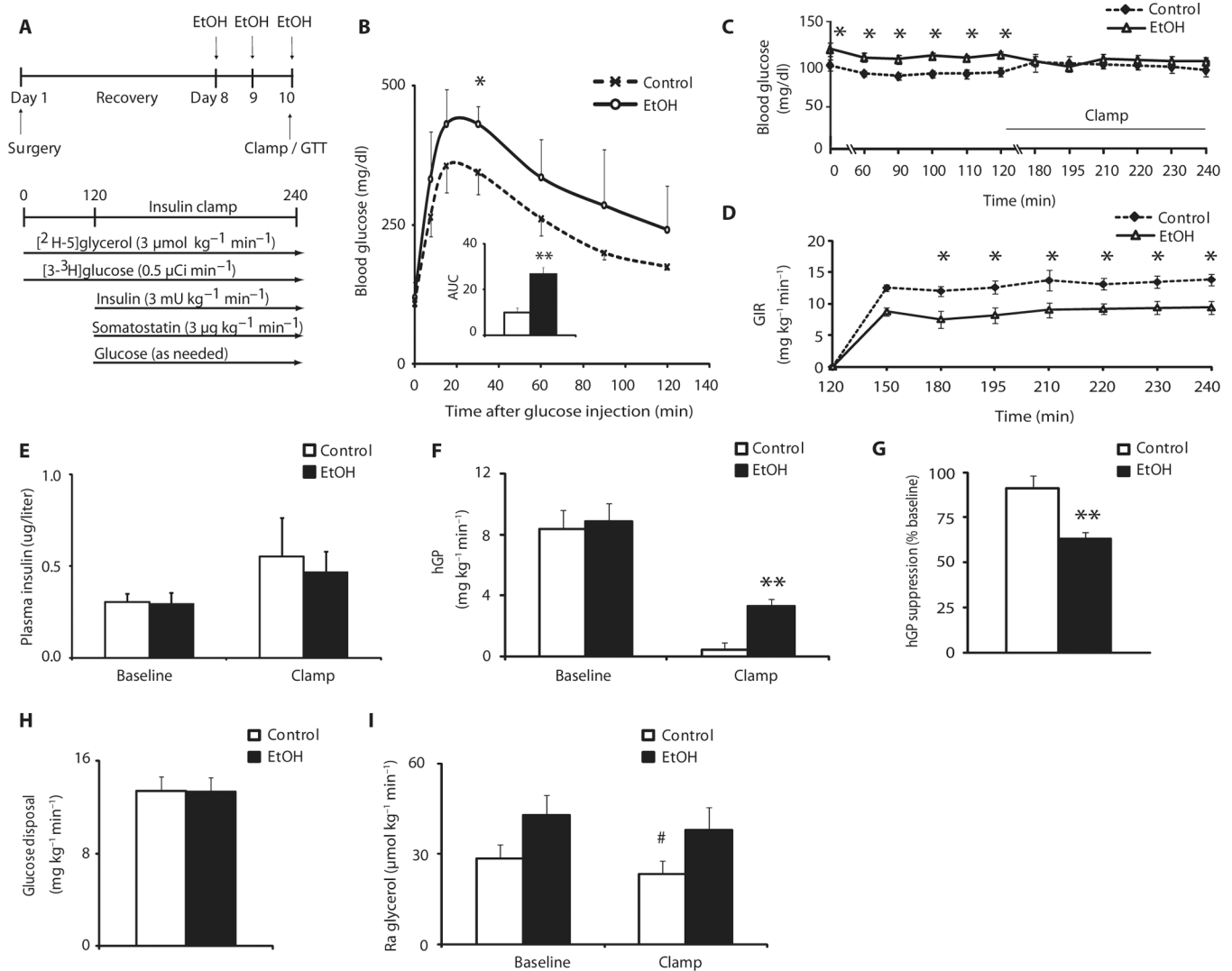


Fig. 1. Binge drinking disrupts glucose homeostasis by impairing insulin action in liver and adipose tissue. Female rats were treated with isocaloric glucose (control) or ethanol and subjected to hyperinsulinemic (3mU) pancreatic clamp studies. **(A)** Scheme showing binge drinking model and experimental protocol of the hyperinsulinemic pancreatic clamp studies. **(B)** Blood glucose concentrations during a GTT (2g/kg) in female rats treated intraperitoneally with saline or ethanol (EtOH). Inset, area under the curve (AUC) ($n = 4$ per group). **(C)** Blood glucose during baseline and clamp in control or ethanol-treated female rats ($n = 9$ control group, $n = 8$ ethanol group). **(D)** GIR needed during the clamp to maintain euglycemia in control or ethanol-treated female rats ($n = 9$ control group, $n = 8$ ethanol group). **(E)** Plasma insulin concentrations during baseline and clamped conditions in control or ethanol-treated female rats ($n = 9$ control group, $n = 8$ ethanol group). **(F)** hGP during baseline and clamped conditions in control or ethanol-treated female rats ($n = 9$ control group, $n = 8$ ethanol group). **(G)** hGP expressed as percentage (%) of suppression from baseline during the clamp in control or ethanol-treated female rats ($n = 9$ control group, $n = 8$ ethanol group). **(H)** Glucose disposal during clamp in control or ethanol-treated female rats ($n = 9$ control group, $n = 8$ ethanol group). **(I)** Ra glycerol during baseline and clamped conditions in control or ethanol-treated female rats ($n = 9$ control group, $n = 8$ ethanol

group). * $P < 0.05$; ** $P < 0.01$, control versus ethanol group; # $P < 0.01$, control baseline versus control insulin clamp, per two-tailed unpaired Student's t test (B, C, D, G, and H) or two-way analysis of variance (ANOVA) followed by Bonferroni posttest (E, F, and I).

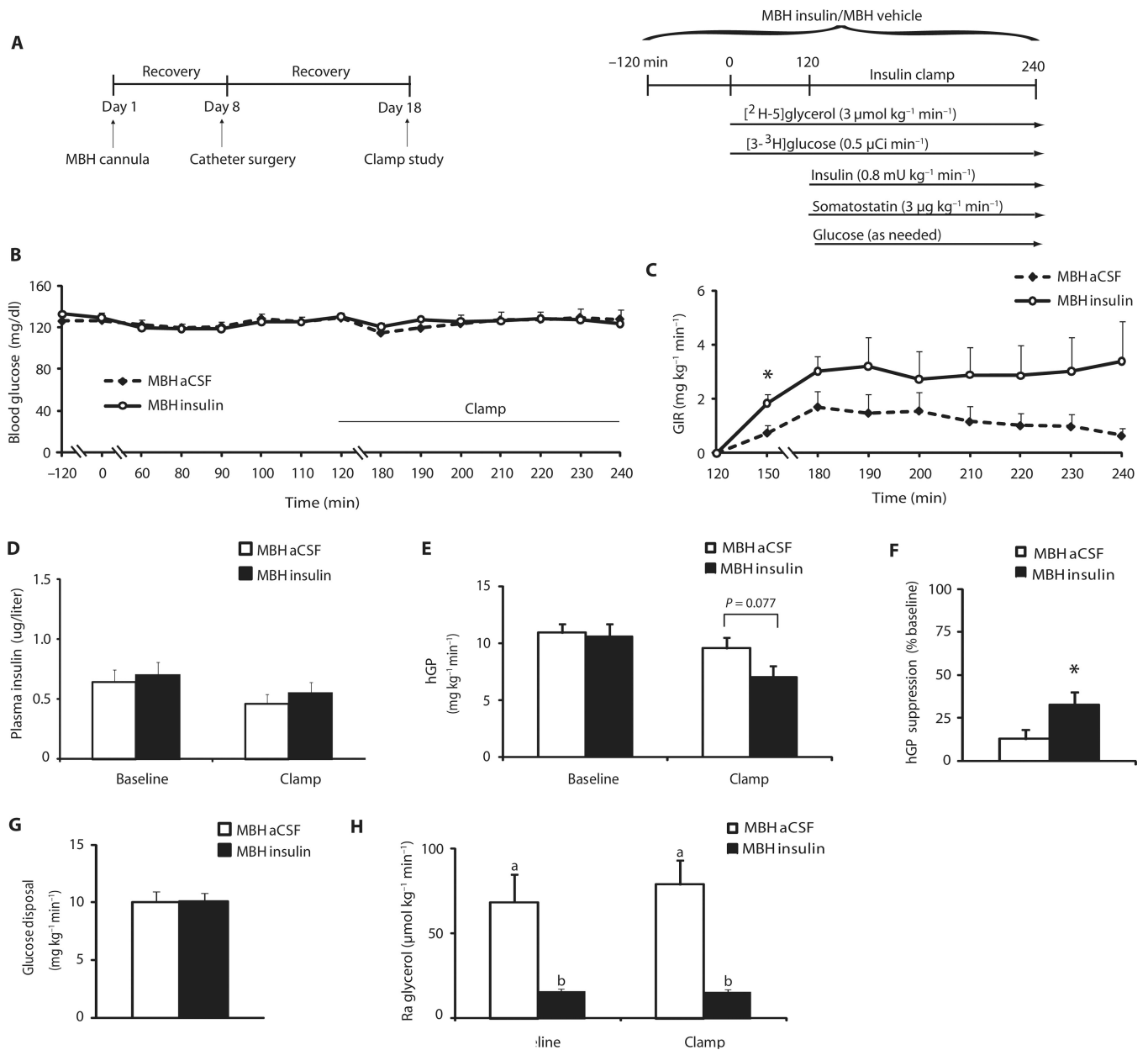


Fig. 2. MBH insulin suppresses hGP and WAT lipolysis in female rats. Female rats were infused with vehicle (aCSF) or insulin into the MBH, whereas insulin concentrations were maintained at basal values. (A) Scheme and experimental protocol of experiments testing the effect of hypothalamic insulin infusions on hepatic and adipose tissue function measured by pancreatic clamp studies. (B) Blood glucose during baseline and the clamp in vehicle (aCSF)- or insulin-infused female rats ($n = 9$ per group). (C) GIR needed during the clamp to maintain euglycemia in vehicle- or insulin-infused female rats ($n = 9$ per group). (D) Plasma insulin concentrations during baseline and clamped conditions in vehicle- or insulin-infused female rats ($n = 9$ per group). (E) hGP during baseline and clamped conditions in vehicle- or insulin-infused female rats ($n = 9$ per group). (F) hGP expressed as percentage (%) of suppression from baseline during the clamp in vehicle- or insulin-infused female rats ($n = 9$ per group). (G) Glucose disposal during the insulin clamp in vehicle- or insulin-

infused female rats ($n = 9$ per group). (**H**) Ra glycerol during baseline and clamped conditions in vehicle- or insulin-infused female rats ($n = 9$ per group). * $P < 0.05$, vehicle-versus insulin-infused rats, per two-tailed unpaired Student's t test (B, C, E, F, and G) or two-way ANOVA followed by Bonferroni posttest (D, E, and H). Bars that do not share the same letter are significantly ($P < 0.05$) different from each other, per two-tailed unpaired Student's t test.

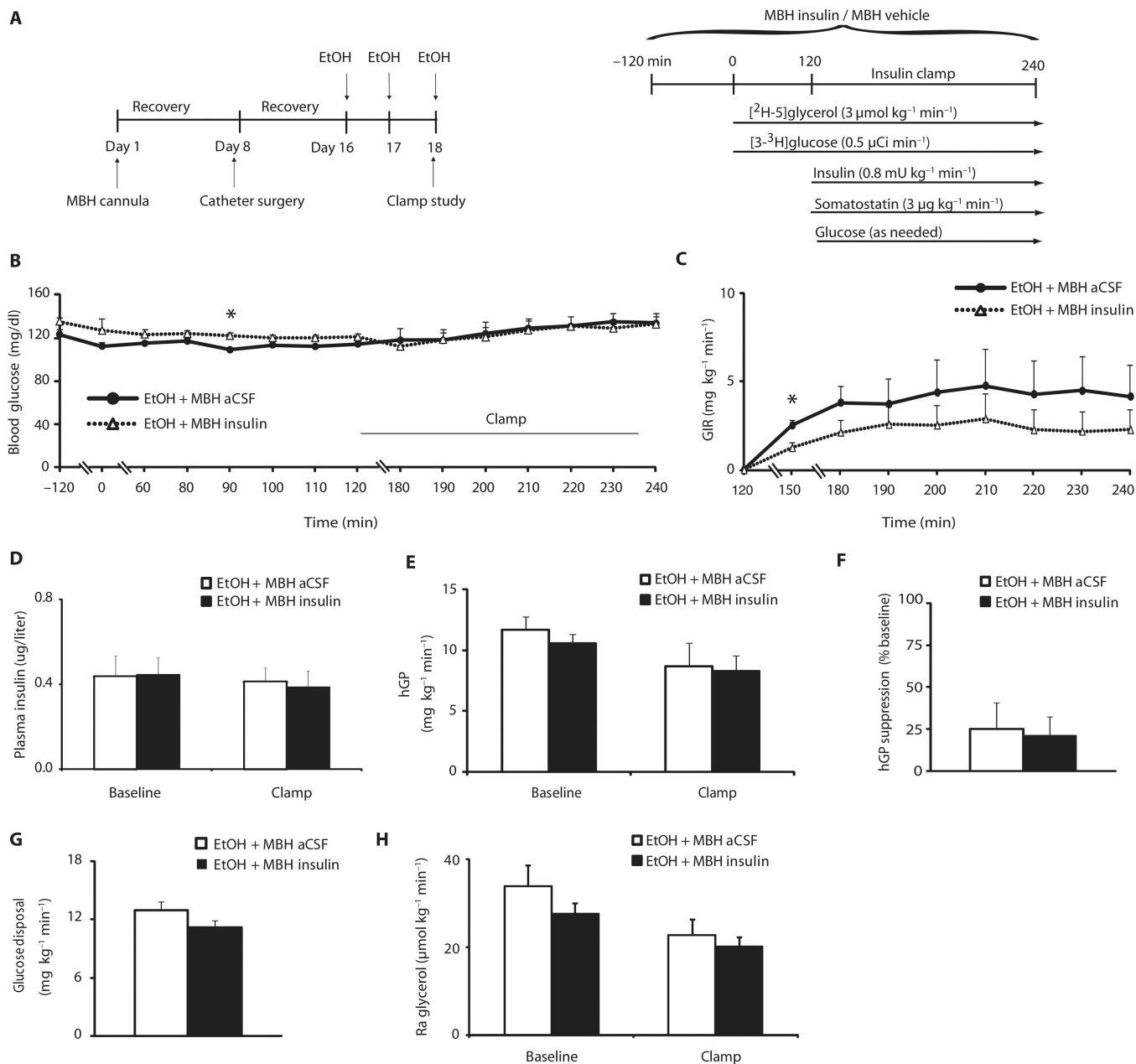


Fig. 3. Binge drinking eliminates hypothalamic insulin action. Female rats were treated with ethanol for three consecutive days and then infused with either vehicle (aCSF) or insulin into the MBH while maintaining insulin concentrations at basal values. **(A)** Scheme and experimental protocol of binge drinking model and pancreatic clamp studies combined with central infusions. **(B)** Blood glucose during baseline and clamp in vehicle (aCSF)- or insulin-infused and ethanol-treated female rats ($n = 7$ MBH aCSF/ethanol group, $n = 6$ MBH insulin/ethanol group). **(C)** GIR needed during the clamp to maintain euglycemia in vehicle- or insulin-infused and ethanol-treated female rats ($n = 7$ MBH aCSF/ethanol group, $n = 6$ MBH insulin/ethanol group). **(D)** Plasma insulin concentrations during baseline and clamped conditions in vehicle- or insulin-infused and ethanol-treated female rats ($n = 7$ MBH aCSF/ethanol group, $n = 6$ MBH insulin/ethanol group). **(E)** hGP during baseline and clamped

conditions in vehicle- or insulin-infused and ethanol-treated female rats ($n = 7$ MBH aCSF/ethanol group, $n = 6$ MBH insulin/ethanol group). **(F)** hGP expressed as percentage (%) of suppression from baseline during the clamp in vehicle- or insulin-infused and ethanol-treated female rats ($n = 7$ MBH aCSF/ethanol group, $n = 6$ MBH insulin/ethanol group). **(G)** Glucose disposal during the clamp in vehicle- or insulin-infused and ethanol-treated female rats ($n = 7$ MBH aCSF/ethanol group, $n = 6$ MBH insulin/ethanol group). **(H)** Ra glycerol during baseline and clamped conditions in vehicle- or insulin-infused and ethanol-treated female rats ($n = 7$ MBH aCSF/ethanol group, $n = 6$ MBH insulin/ethanol group). * $P < 0.05$, control versus ethanol group, per two-tailed unpaired Student's t test (B, C, E, F, and G) or two-way ANOVA followed by Bonferroni posttest (D, E, and H). Bars that do not share the same letter are significantly ($P < 0.05$) different from each other, per two-tailed unpaired Student's t test.

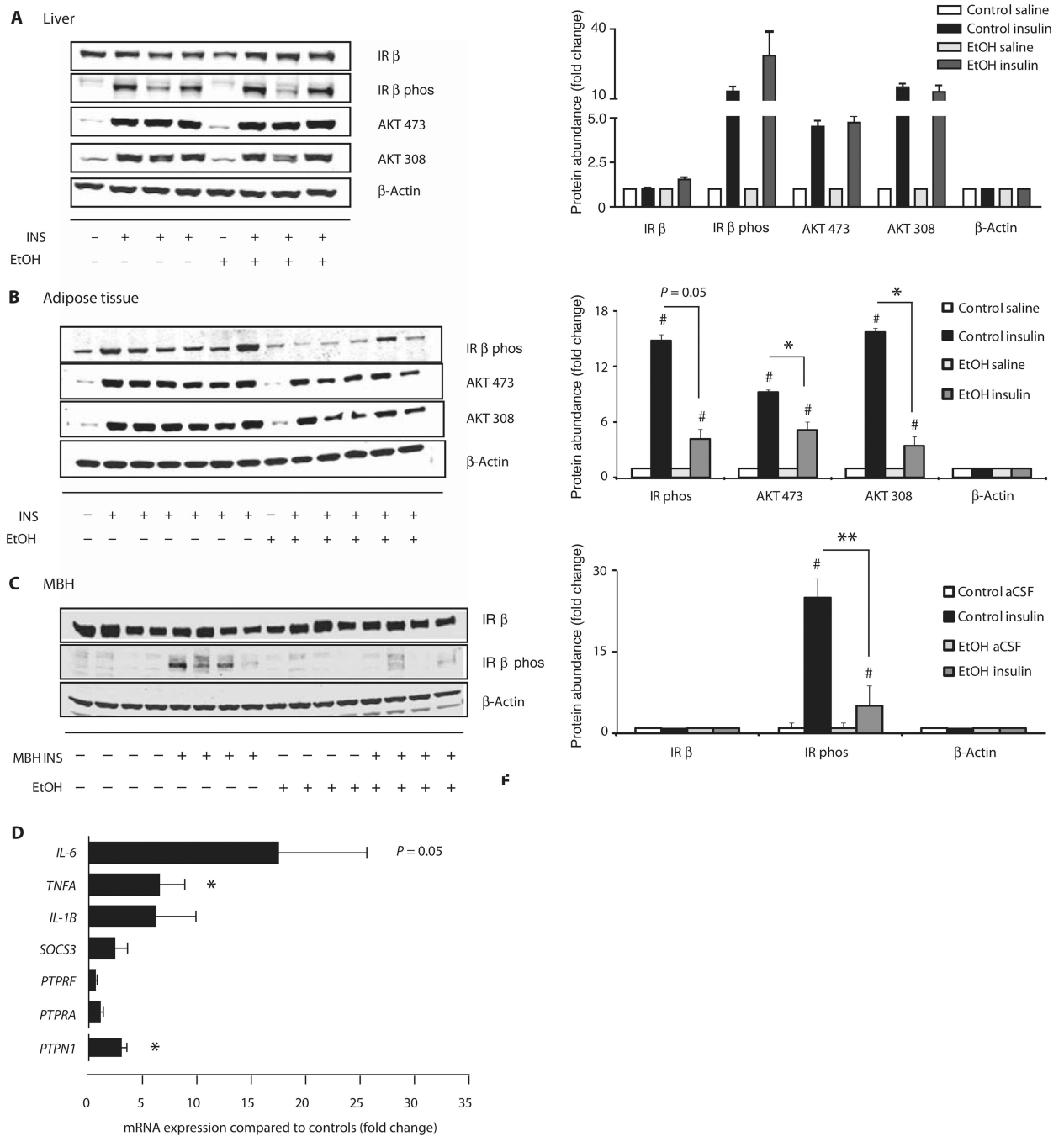


Fig. 4. Binge drinking impairs insulin signaling in vivo in MBH and adipose tissue and increases inflammation and PTP1B. Female rats were treated with isocaloric glucose (control) or ethanol, and insulin signaling in liver, adipose tissue, and MBH was assessed by Western blot. **(A)** Effect of binge drinking on insulin signaling in liver. Left, representative Western blot; right, quantification of Western blot ($n = 1$ control/saline, $n = 1$ ethanol/saline, $n = 3$ control/insulin, $n = 3$ ethanol/insulin). **(B)** Effect of binge drinking on insulin signaling in epigonadal adipose tissue. Left, representative Western blot; right, quantification of Western blot ($n = 1$ control/saline, $n = 1$ ethanol/saline, $n = 3$ control/insulin, $n = 3$ ethanol/insulin).

(C) Effect of binge drinking on insulin signaling in the MBH. Left, representative Western blot; right, quantification of Western blot ($n = 4$ control/saline, $n = 4$ ethanol/saline, $n = 4$ control/insulin, $n = 4$ ethanol/insulin). (D) Inflammatory cytokines and tyrosine receptor phosphatases as assessed by quantitative real-time polymerase chain reaction (qRT-PCR) in the MBH of rats treated with control or ethanol ($n = 6$ control group, $n = 5$ ethanol group, $n = 4$ per group for PTPN1). * $P < 0.05$, ** $P < 0.01$, control versus ethanol group; # $P < 0.05$, unstimulated control versus stimulated control and unstimulated ethanol versus stimulated ethanol, per two-tailed unpaired Student's t test. Bars represent insulin-treated samples normalized to β -actin and unstimulated samples.

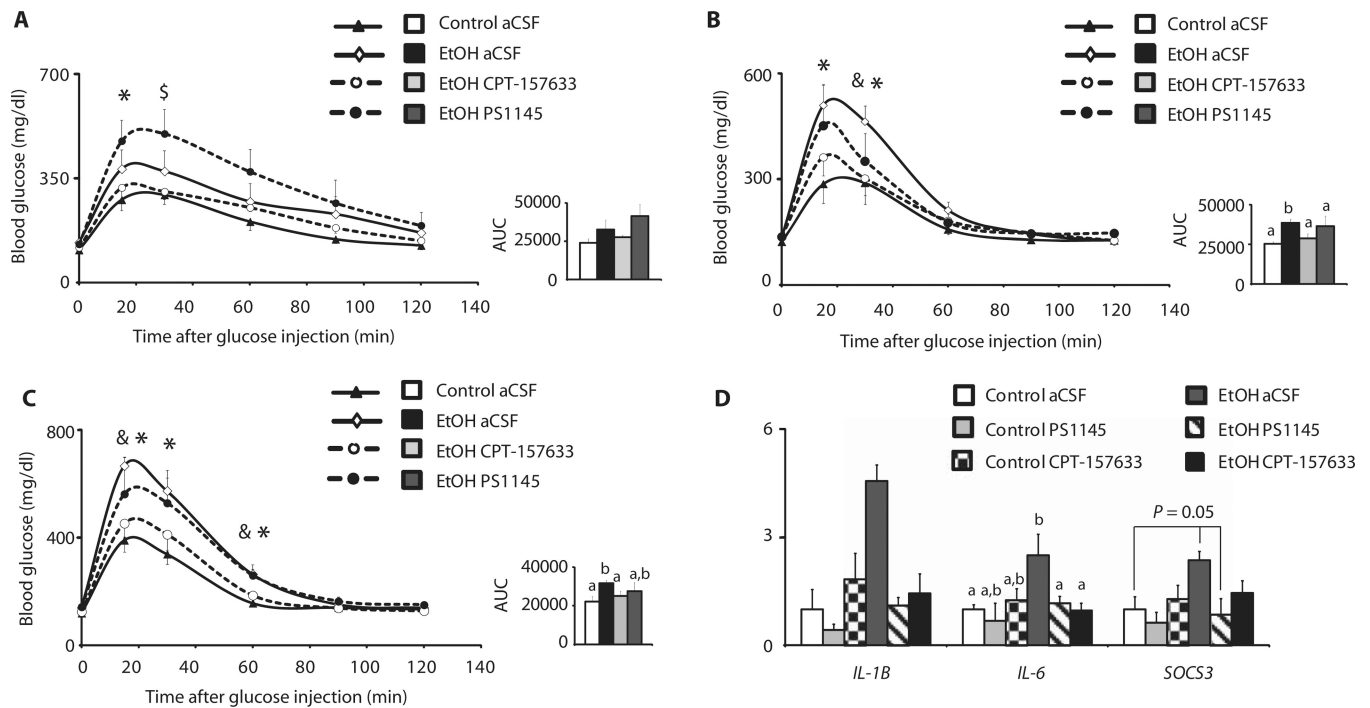


Fig. 5. Inhibition of PTP1B in the MBH restores glucose tolerance after binge drinking. Female rats were treated with either isocaloric glucose (control) or ethanol and were centrally infused with an IKK β inhibitor (PS1145), a PTP1B inhibitor (CPT-157633), or vehicle and subjected to GTTs [glucose (3 g/kg)]. (A to C) Eight to 10 hours (A), 30 hours (B), and 54 hours (C) after the last dose of ethanol. Left panels, blood glucose concentrations after glucose injection; right panels, AUC ($n = 5$ control/aCSF, $n = 5$ ethanol/aCSF, $n = 4$ ethanol/PS1145, $n = 7$ ethanol/CPT-157633). (D) Inflammatory cytokines as assessed by qRT-PCR in the MBH of rats that were treated with control or ethanol and were continuously infused with PS1145 or CPT-157633 ($n = 4$ control/aCSF, $n = 3$ control/PS1145, $n = 4$ control/CPT-157633, $n = 4$ ethanol/aCSF, $n = 3$ ethanol/PS1145, $n = 4$ ethanol/CPT-157633). * $P < 0.05$, control/aCSF versus ethanol/aCSF; \$ $P < 0.05$, control/aCSF versus ethanol/PS1145; # $P < 0.05$, control/aCSF versus ethanol/CPT-157633; & $P < 0.05$, ethanol/aCSF versus ethanol/CPT-157633. Bars that do not share the same letter are significantly ($P < 0.05$) different from each other, per two-tailed unpaired Student's t test.

Table 1

Body weights of female rats before and after surgery on the day of the experiment. Values are presented as means \pm SEM. * $P < 0.05$, per two-tailed unpaired Student's t test. i.p., intraperitoneal.

Group	Presurgical (g)	<i>n</i>	Postsurgical (g)	<i>n</i>
Hyperinsulinemic (3 mU) clamp/control	251 \pm 9.4	9	231 \pm 9.4	9
Hyperinsulinemic (3 mU) clamp/ethanol	247 \pm 12.7	8	230 \pm 18.5	8
Hyperinsulinemic (3 mU) clamp/control 30 hours after last i.p. injection	230 \pm 8.32	7	224 \pm 10.57	7
Hyperinsulinemic (3 mU) clamp/ethanol 30 hours after last i.p. injection	234 \pm 5.75	8	231 \pm 8.17	8
Basal clamp (0.8 mU) MBH aCSF without ethanol	245 \pm 19.5	9	241 \pm 17.5	9
Basal clamp (0.8 mU) MBH insulin without ethanol	244 \pm 14.6	9	246 \pm 18.9	9
Basal clamp (0.8 mU) MBH aCSF/ethanol	230 \pm 12.3	7	227 \pm 9.0	7
Basal clamp (0.8 mU) MBH insulin/ethanol	229 \pm 14.1	6	230 \pm 8.1	6